Silicon(IV) Chelates of an (*ONN′*)-Tridentate Pyrrole-2-Carbaldimine Ligand: Syntheses, Structures and UV/Vis Properties

Daniela Gerlach[a], Andreas W. Ehlers[b], Koop Lammertsma[b], and Jörg Wagler[a]

[a] Institut für Anorganische Chemie, Technische Universität Bergakademie Freiberg, Leipziger Straße 29, 09596 Freiberg, Germany
[b] Department of Chemistry, Faculty of Sciences, Vrije Universiteit Amsterdam, De Boelelaan 1083, 1081 HV Amsterdam, The Netherlands

Reprint requests to Dr. Jörg Wagler. Fax: (+49) 3731 39 4058.
E-mail: joerg.wagler@chemie.tu-freiberg.de

Z. Naturforsch. **2009**, *64b,* 1571 – 1579; received September 14, 2009

Dedicated to Professor Hubert Schmidbaur on the occasion of his 75th birthday

The tridentate (*ONN′*)-chelator properties of the pyrrole-2-(*o*-hydroxyphenyl)carbaldimine dianion (L^{2-}) were explored for the neutral penta-coordinate diorganosilicon complexes LSiRR′ (R,R′ = Ph, Ph; Ph, Me; Ph, *t*Bu) where the ligand L occupies the ax-eq-ax sites in a distorted trigonal-bipyramidal arrangement arround the silicon atom, and for the neutral hexa-coordinate L_2Si, that has a *mer*-coordination. Single-crystal X-ray diffraction analyses show an almost planar ligand backbone with a Si–N bond to the imine group that is shorter in hexa-coordinate L_2Si than in penta-coordinate LSiRR′. In sharp contrast to the almost colorless neutral ligand LH_2, both complexes show pronounced UV/Vis absorptions in the red-brown region that originate from HOMO - LUMO and HOMO-1 - LUMO transitions, and that are due to intra-ligand π-π^* transitions from the *N*-*o*-oxyphenylimine towards the imine moiety.

Key words: Chelate, Time-dependent DFT, Hypercoordination, Pyrrole, Schiff Base, UV/Vis

Introduction

Silicon compounds with a silicon coordination number of five or six [1, 2] are of interest for their enhanced reactivity [3] and electronic properties [4]. Of the many ligands that are explored for their coordination behavior to silicon, our focus is on the tridentate *ONN′*-chelators and in particular on the doubly deprotonated 2-(*N*-2-hydroxyphenyl)pyrrolcarbaldimine (LH_2) [5]. This tridentate chelator can in principle occupy different coordination sites of the trigonal-bipyramidal silicon coordination sphere, as shown for the neutral compounds $LSi(CH_2)_3$ and LSiPhMe (Scheme 1) [5d].

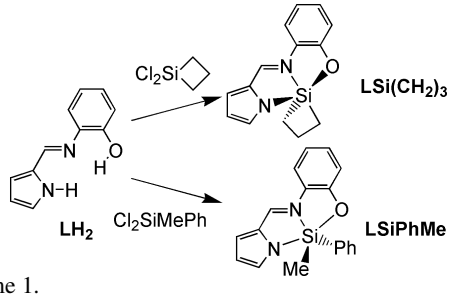

Scheme 1.

Relatively little is known about the coordinative abilities of the L^{2-} ligand [8], except in transition metal complexes of copper, nickel, rhodium, iridium and rhenium [6], some of which have found use as catalysts in the polymerization of ethylene and α-olefins [7]. In the present study we focus on the intriguing flexibility of this ligand in the coordination sphere of silicon.

Results and Discussion

The 2-(*N*-2-hydroxyphenyl)pyrrolcarbaldimine dianion acts as a tridentate (*ONN′*)-chelator in the neutral penta-coordinate LSiPhMe that carries two additional C substituents [5d]. The imine group gives an unexpectedly short N–Si bond whereas that resulting from the deprotonated pyrrole is slightly longer. To explore whether this behavior relates to steric congestion around the silicon atom, novel penta-coordinate Si complexes were synthesized from the neutral ligand LH_2 and the diorganodichlorosilanes Cl_2SiRR' (R,R′ = Me, Me; Cy, Me; Ph, tBu; Ph, Cy; Ph, Ph) (Scheme 2).

R	R′	δ
Me	Me	−62.2
Cy	Me	−62.3
Ph	*t*Bu	−72.2
Ph	Me	−74.1
Ph	Cy	−75.7
Ph	Ph	−85.5

Table 1. Selected ^{29}Si NMR chemical shifts δ (in ppm relative to $SiMe_4$) of penta-coordinate silicon complexes LSiRR′.

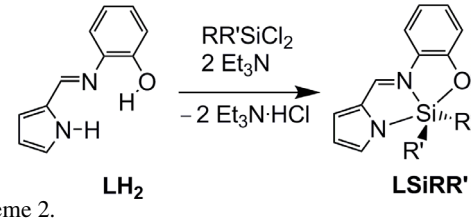

Scheme 2.

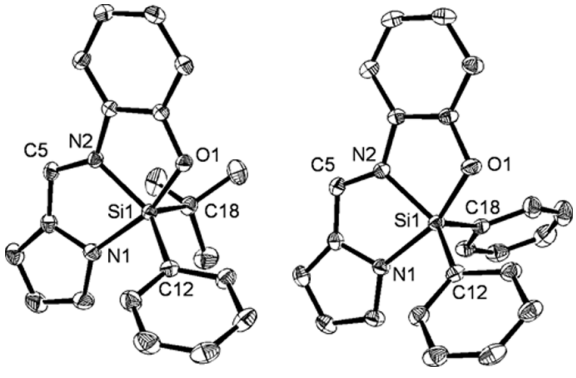

Fig. 1. Molecular structure of LSiPh*t*Bu (left; only one of the two independent molecules in the asymmetric unit is shown) and $LSiPh_2$ (right). (ORTEP; displacement ellipsoids at the 20 % probability level; hydrogen atoms omitted for clarity).

All complexes LSiRR′ were analyzed by ^{29}Si NMR spectroscopy (Table 1). The observed chemical shift depends on the nature of the two carbon substituents and is at higher field in the order alkyl/alkyl < alkyl/aryl < aryl/aryl. Within each of the three sets, the chemical shifts are very similar, thereby suggesting also a similar coordination for the *ONN′*-ligand. This was confirmed by single crystal X-ray diffraction analyses for the complexes LSiPh*t*Bu and $LSiPh_2$ (Fig. 1) that compare well with the earlier reported structure for LSiPhMe (Table 2) [5d].

The molecular structures of the three complexes all show the Si1–N1 bond to the pyrrole to be slightly longer than the Si1–N2 bond to the imine. This difference might be due to the axial *versus* equatorial coordination of the penta-coordinate silicon, but Schilde *et al.*, who reported on a comparable Re(V) complex, attributed the difference to electron pushing of the

Table 2. Selected bond lengths (Å) for LSiPh*t*Bu, LSiPhMe, and $LSiPh_2$ with estimated standard deviations in parentheses.

	LSiPh*t*Bu	**LSiPhMe**	**$LSiPh_2$**
Si1–O1	1.791(2)	1.776(2)	1.781(2)
Si1–N1	1.926(2)	1.923(2)	1.905(2)
Si1–N2	1.883(2)	1.897(2)	1.890(2)
Si1–C18	1.906(2)	1.867(2)	1.885(2)
Si1–C12 (Ph)	1.890(2)	1.885(2)	1.892(2)

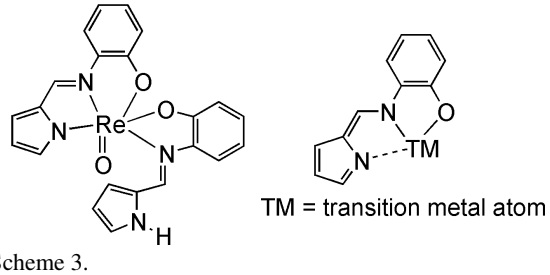

Scheme 3.

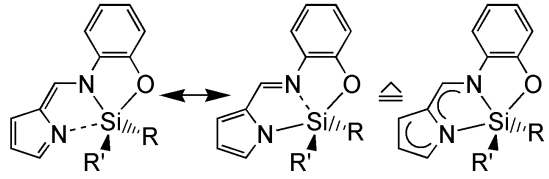

Scheme 4.

pyrrole ring (Scheme 3, right) [6d]. The three complexes LSiPh*t*Bu, LSiPhMe, and $LSiPh_2$ further reveal that their respective C5–N2 imine bond length of 1.309(2), 1.306(2), and 1.310(2) Å, is longer than in LH_2 (1.283(2) Å). This elongation of the imine bond suggests relevant contributions from the canonical forms depicted in Scheme 4 or – in other words – the tridentate ligand acts as an extended π system.

Steric factors underlie the differences in the Si–C bond lengths. For example, the Si–C bond to the *t*Bu group in LSiPh*t*Bu is much longer than that to the phenyl and methyl groups in LSiPhMe and $LSiPh_2$. The three distorted trigonal-bipyramidal systems with the oxygen and pyrrole nitrogen atoms in axial positions also show a remarkable flexibility of the ONN′ ligand in the silicon coordination sphere, as is particularly evident from the differences in the equatorial A–Si–B angles (especially in case of the two crystallographically independent molecules for LSiPh*t*Bu, Table 3). The equatorial N2–Si1–C12 angle differs by up to 5.6° in the two independent molecules of LSiPh*t*Bu and by up to 23.2° in the three different complexes, possibly due to the lower steric demand of the methyl group in LSiPhMe. In contrast, the axial O1–Si1–N1

Table 3. Selected bond angles (deg) for LSiPh*t*Bu, LSiPhMe and $LSiPh_2$ with estimated standard deviations in parentheses.

	LSiPh*t*Bu	LSiPhMe	$LSiPh_2$
N2–Si1–C18	108.7(1) / 111.5(1)	135.2(1) / 136.6(1)	111.1(1)
N2–Si1–C12	133.9(1) / 128.3(1)	111.2(1) / 110.2(1)	134.4(1)
C18–Si1–C12	117.4(1) / 120.2(1)	113.6(1) / 113.2(1)	114.5(1)
O1–Si1–N1	158.1(1) / 160.1(1)	160.8(1) / 159.8(1)	161.2(1)

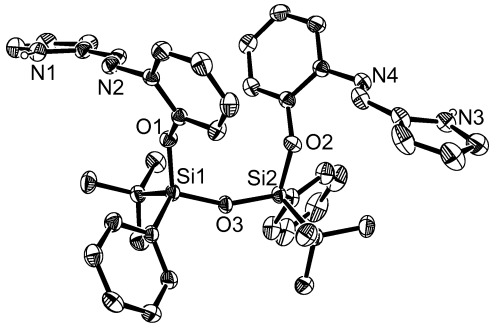

Fig. 2. Molecular structure of (LH)Ph*t*BuSi-O-SiPh*t*Bu(LH). (ORTEP; displacement ellipsoids at the 20 % probability level; C-bound hydrogen atoms omitted for clarity.)

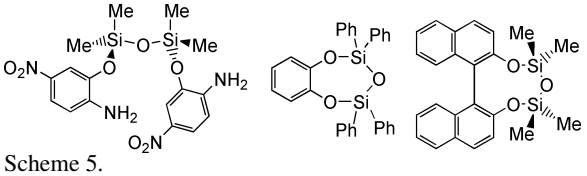

Scheme 5.

angle is essentially the same for all three complexes, probably due to the almost planar arrangement of the tridentate ligand. This then seems to suggest that the radius of the silicon atom determines the depth of SiRR′ insertion into the ligand clamp.

The synthesis of LSiPh*t*Bu also gave a small amount of (LH)Ph*t*BuSi-O-SiPh*t*Bu(LH) as by-product. Its molecular structure (Fig. 2), obtained by a single crystal X-ray diffraction analysis, reveals a disiloxane with singly deprotonated ligands (LH^-) that are attached to the Si atom only by the phenoxy oxygen atoms. This suggests that double deprotonation is needed for the ligand to coordinate its imine nitrogen to the diorganosilicon moiety. The two crystallographically independent molecules exhibit an arrangement comparable to that of the copper complexes reported by Castro *et al.* [6a]. Molecular structures of similar disiloxanes with a [C_2(ArO)]-Si-O-Si-[(O-Ar)C_2] backbone have been described of which the open-chain disiloxane by Jiang *et al.* (Scheme 5, left) [9] shows a notably wider Si–O–Si angle (160.7(1)°) than the cyclic siloxanes reported by Hanson *et al.* [10] [135.0(1)°, (Scheme 5; middle)] and Liu *et al.* [11] [151.2(1)°, (Scheme 5, right)] and than that observed in (LH)Ph*t*BuSi-O-SiPh*t*Bu(LH) (156.1(1)°).

	$LSiPh_2$	L_2Si
Si–N_P	1.905(1)	1.894
Si–N_I	1.890(1)	1.867
Si–O	1.781(1)	1.768
N=C	1.310(2)	1.309

Table 4. Selected bond lengths (Å) of $LSiPh_2$ and L_2Si (average of all four molecules for L_2Si); (N_P = nitrogen atom in the pyrrolic system, N_I = imine nitrogen atom).

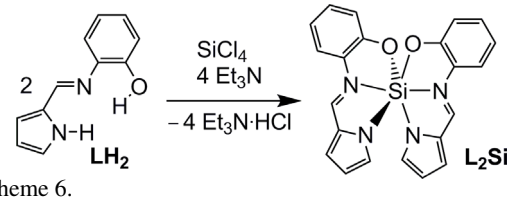

Scheme 6.

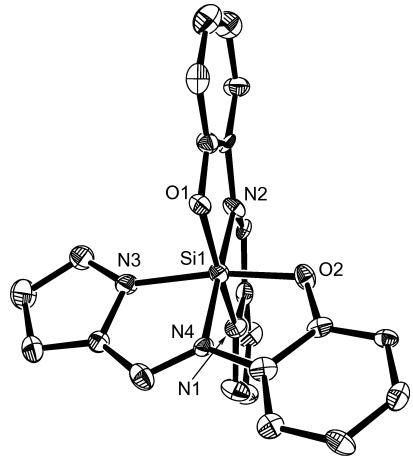

Fig. 3. Molecular structure of one of the four crystallographically independent molecules of L_2Si (ORTEP; displacement ellipsoids at the 50 % probability level; hydrogen atoms omitted for clarity). Selected bond lengths (Å): Si1–O1 1.768(5), Si1–O2 1.776(5), Si1–N2 1.886(6), Si1–N4 1.864(6), Si1–N1 1.887(6), Si1–N3 1.905(6), N2–C5 1.280(8), N4–C16 1.325 (8).

The synthesis of $LSiCl_2$ was attempted to expand the series of penta-coordinate LSiRR′ complexes with halogen substituents. However, the reaction of the tridentate ligand L^{2-} with $SiCl_4$ resulted in the formation of the hexa-coordinate silicon chelate L_2Si (Scheme 6) that has a characteristic ^{29}Si NMR chemical shift at −160.4 ppm. Brown crystals of L_2Si could be obtained that were suitable for a single crystal X-ray diffraction analysis (Fig. 3).

A comparison of the bond lengths of L_2Si with those of $LSiPh_2$ (Table 4) surprisingly shows that despite its higher silicon coordination number, all Si–N and Si–O bonds in L_2Si are shorter than those in penta-

coordinate $LSiPh_2$. Apparently, replacement of the two phenyl substituents by a ligand with three electronegative binding sites enhances the Lewis acidity of the Si atom. The largest difference is found for the Si–N_I bond (0.023Å). This behavior is in accord with recent findings by Seiler *et al.* [12]. Because of the planarity of the tridentate ligand L^{2-} the ax-eq-ax positions of the distorted trigonal bipyramid are occupied in $LSiPh_2$, while a *mer* arrangement results for L_2Si.

All penta-coordinate complexes are intensely red, and the origin of the color was examined by analysis of the UV/Vis spectra of LSiPh*t*Bu, LSiPhMe and $LSiPh_2$. Upon complex formation with a diorganosilicon moiety both bands of the pale-yellow ligand LH_2 ($\lambda_{max\,1}$ = 307, $\lambda_{max\,2}$ = 357 nm) undergo large bathochromic shifts, particularly the second one, as is shown in Fig. 4 for $LSiPh_2$ ($\lambda_{max\,1}$ = 352, $\lambda_{max\,2}$ = 470 nm), while the molar extinction decreases significantly only for the first band (LH_2: ε_1 = 12700, ε_2 = 24600; $LSiPh_2$: ε_1 = 4690, ε_2 = 19700 $L\,mol^{-1}\cdot cm^{-1}$). If the same interpretation applies that Pettinari *et al.* used to explain the UV/Vis spectra for the related salop Sn(IV) complexes (Scheme 7) [13], then the absorption at 352 nm should be attributed to a $\pi \rightarrow \pi^*$ transition of the benzenoid system and the band at 470 nm to a $\pi \rightarrow \pi^*$ transition of the imine-bridged conjugated π system. At first sight this interpretation seems reasonable as the change for the benzenoid system on going from LH_2 to $LSiPh_2$ is expected to be only small on replacing a phenoxy proton by a "Si^+" ion, while that for the imine group is substantial on coordination of the nitrogen lone pair, but there are also indications that this interpretation is flawed.

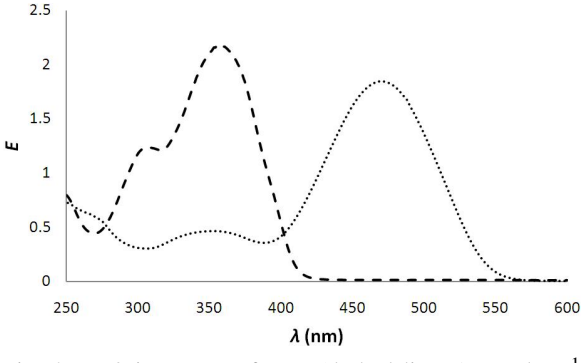

Fig. 4. UV/Vis spectra of LH_2 (dashed line; 1 mmol L^{-1} and 1 mm) and $LSiPh_2$ (dotted line; 1 mmol L^{-1} and quartz cuvettes d = 1 mm); $E = \log(I_0/I)$.

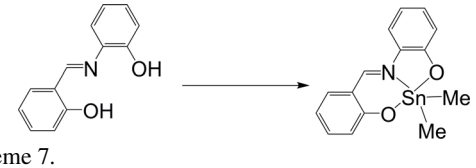

Scheme 7.

The comparable UV/Vis characteristics of $LSiRR'$ and the salop Sn(IV) complexes can be considered as a result of both the similar donor-atom situation *N*-(*o*-oxyphenylimine) and a planar arrangement of the tridentate ligand, which gives rise to an extended π system. That the red shift of band 1 is related to the planarity of the ligand was earlier demonstrated by one of us for salop silicon complexes. For example, structure **A** (R, R = Me, Silyl) in Scheme 8 has a planar *ONO'*-ligand and absorbs at 464 nm, while **B** (R, R = Ph, Ph) with a twisted ligand absorbs at 386 nm [14]. Although the planarity of the *ONN'*-ligand would suggest an influence of the pyrrole ring on the extended π system and hence on the optical properties of $LSiRR'$, its definite role remains unclear. Interaction of the pyrrole ring with the imine group is expected to cause an intramolecular charge transfer. However, the influence of different solvents on the second absorption band of $LSiPh_2$ was found to be marginal, *i. e.*, 458.0 nm in acetonitrile, 463.0 nm in THF, 468.7 nm in toluene, and 470.4 nm in chloroform (Fig. 5), which indicates that polar effects do not contribute significantly and raises the concern whether this absorption band is properly attributed to the $\pi \rightarrow \pi^*$ transition of the conjugated C=N-bridged system.

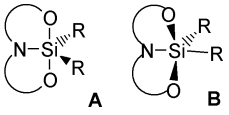

Scheme 8.

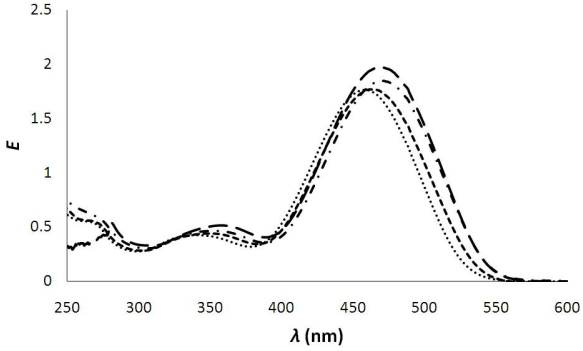

Fig. 5. UV/Vis spectra of $LSiPh_2$ in (left to right) acetonitrile, THF, toluene, chloroform; c = 1 mmol L^{-1}; d = 1 mm; $E = \log(I_0/I)$.

Table 5. Singlet transitions calculated for LH_2 and $LSiPh_2$ using TD DFT B3LYP/6-311+G(d,p).[a]

Excited state	Transition	c[b]	E (eV)	λ (nm)	f[c]
LH_2					
1	HOMO → LUMO	0.61738	3.3612	368.9	0.5031
	HOMO-1 → LUMO	−0.19011			
2	HOMO → LUMO	0.13735	3.9760	311.8	0.2668
	HOMO-1 → LUMO	0.63669			
	HOMO-2 → LUMO	0.10671			
$LSiPh_2$					
1	HOMO → LUMO	0.63031	2.6908	460.8	0.2463
	HOMO-1 → LUMO	0.14950			
2	HOMO-1 → LUMO	0.64472	3.4087	363.7	0.1811

[a] The energies of the HOMO-1, HOMO and LUMO (a. u.) are, respectively, −0.238, −0.210, and −0.074 for LH_2, and −0.225, −0.197, and −0.080 for $LSiPh_2$; [b] c = coefficient of the wave function for each excitation; [c] f = oscillator strength.

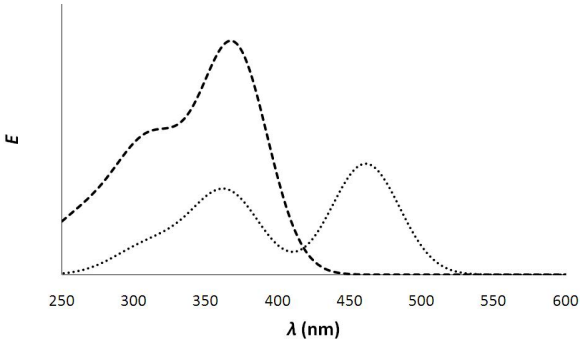

Fig. 6. UV/Vis spectra simulated for LH_2 (dashed line) and $LSiPh_2$ (dotted line) using TD DFT on the B3LYP/6-311+G(d,p) level.

In oder to analyze the origin of both observed absorption bands in more detail time-dependent DFT calculations were performed. The molecular structures of LH_2 [5d] and $LSiPh_2$ were optimized with B3LYP/6-31G(d) and subsequently analyzed by TDDFT for singlet transitions at B3LYP/6-311G+(d,p) using eight excited states. These computations predict indeed two strong absorption bands for both LH_2 and $LSiPh_2$, as summarized in Table 5. The simulated spectra displayed in Fig. 6 agree remarkably well with the experimentally obtained spectra shown in Fig. 4 with a $\Delta\lambda_{max}$ of only 12 nm, and also the relative intensities compare well, although only qualitatively.

The UV/Vis absorption bands for the two compounds appear to have the same origin. The HOMO – LUMO transition is the predominant contributor for the lowest energy band and the HOMO-1 – LUMO transition for the other band. The surprisingly strong red shift observed on going from LH_2 to $LSiPh_2$ is mainly due to the elevation of the HOMO and

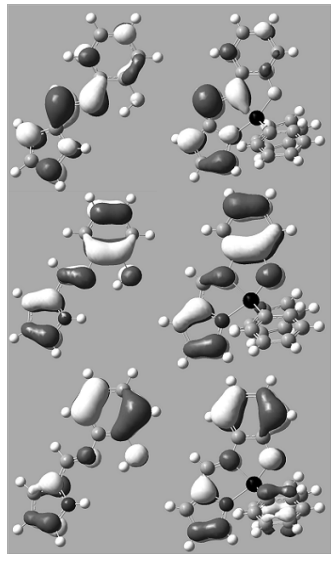

Fig. 7. From top: LUMO, HOMO and HOMO-1 of LH_2 (left) and $LSiPh_2$ (right), isosurface: 0.04.

HOMO-1 energies of $LSiPh_2$, *i. e.*, 0.013 a. u. relative to the LH_2. Fig. 7 shows the three noted MOs for both LH_2 and $LSiPh_2$. All functional groups contribute to these orbitals except the phenolic group in the LUMOs. Thus, both observed transitions in which the LUMO plays an important role must be interpreted as π-π^* transitions that show only a very modest electron density transfer from the *o*-iminophenol towards the imine moiety.

This MO-based analysis which is in sharp contrast to the interpretation advocated by Pettinari that separates the π-π^* transition of the imine-linked conjugated system (band 2) from the π-π^* transition of the benzenoid system (band 1) may therefore also be applicable to the *N*-(*o*-oxyphenyl)imine-containing Sn complexes [13] and the Si-salop complexes [14].

The same UV/Vis absorptions that are attributable to the pyrrole-2-carbaldimine ligand in $LSiPh_2$ are also found in hexa-coordinate L_2Si, as shown in Fig. 8. Thus, the presence of a second tridentate ligand, and the absence of the carbon substituents, has hardly any effect on the UV/Vis spectrum, thereby underscoring the intra-ligand character of the transition. The very modest blue shift of the high-energy band from 470 nm for $LSiPh_2$ to 464 nm for L_2Si is responsible for the small difference in colors, *i. e.* dark-red for $LSiPh_2$ and brownish-orange for L_2Si. The corresponding blue shift of the low-energy band from 352 to 338 nm for L_2Si is more pronounced and is attributed to the short-

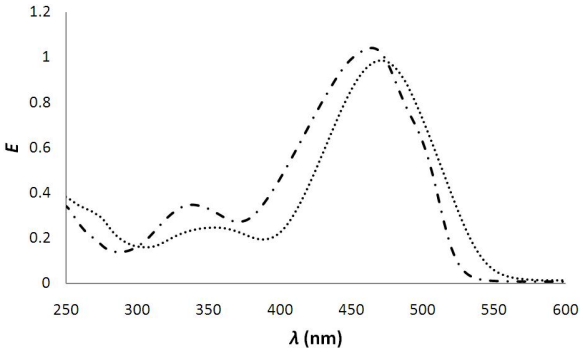

Fig. 8. UV/Vis spectra of $LSiPh_2$ (dotted line, 0.5 mmol L^{-1}) and L_2Si (dashed line, 0.25 mmol L^{-1}) in chloroform; d = 1 mm; $E = \log(I_0/I)$.

ening (*i. e.*, strengthening) of the Si–N and Si–O bonds that is expected to cause a lowering of the HOMO and HOMO-1 levels.

Conclusion

The di-anionic *ONN'*-tridentate ligand L^{2-} prefers the ax-eq-ax positions in a distorted trigonal-bipyramidal arrangement at silicon in the neutral penta-coordinate complexes LSiRR′ (R,R′ = Ph,Ph; Ph,Me; Ph,*t*Bu) and a *mer*-coordination in the neutral hexa-coordinate L_2Si. The UV/Vis characteristics of these compounds are dominated by ligand-based HOMO – LUMO and HOMO-1 – LUMO transitions. Binding of the ligand to silicon causes a significant bathochromic shift of the two observed absorption bands ($LSiPh_2$ *versus* LH_2) due to elevated HOMO and HOMO-1. The time-dependent DFT calculations further show that the observed excitations are accompanied by an electron density transfer from the *N*-(*o*-oxyphenyl)imine towards the imine C=N moiety of the planar ligand.

Experimental Section

All syntheses were carried out in anhydrous solvents under an inert atmosphere of dry argon using standard Schlenk techniques. UV/Vis and NMR spectroscopic analyses were also performed using anhydrous solvents, on a Specord S100 UV/Vis spectrometer and a Bruker DPX 400 NMR spectrometer, respectively. Computational analyses were done with the GAUSSIAN03 software [15].

LSiMe$_2$

A solution of ligand LH_2 (0.25 g, 1.34 mmol) in THF (2.5 mL) was added dropwise to a stirred solution of dimethyldichlorosilane (0.18 g, 1.4 mmol) and triethylamine (0.29 g, 2.9 mmol) in THF (2.5 mL). The red mixture was stirred at ambient temperature for 0.5 h and stored at 4 °C overnight. The precipitate (Et_3NHCl) was filtered off and washed with THF (8 mL). From the filtrate the solvent was removed *in vacuo*, and the residue was dissolved in $CDCl_3$ for ^{29}Si NMR spectroscopic analysis. (Attempts to crystallize $LSiMe_2$, *e. g.*, from diethyl ether or pentane or mixtures thereof, failed so far). – $^{29}Si\{^1H\}$ NMR: $\delta = -62.2$.

LSiCyMe

LSiCyMe was obtained following the procedure described for $LSiMe_2$. Starting materials: Ligand LH_2 (0.36 g, 1.9 mmol) in THF (5 mL); cyclohexylmethyldichlorosilane (0.40 g, 2.0 mmol) and triethylamine (0.59 g, 5.8 mmol) in THF (5 mL). (Attempts to crystallize LSiCyMe, *e. g.*, from diethyl ether or pentane or mixtures thereof, failed so far). – $^{29}Si\{^1H\}$ NMR: $\delta = -62.3$.

LSiPhtBu and (LH)PhtBuSi-O-SiPhtBu(LH)

A solution of LH_2 (0.35 g, 1.9 mmol) THF (5 mL) was added dropwise to a solution of *t*butylphenyldichlorosilane (0.46 g, 2.0 mmol) and triethylamine (0.40 g, 4.0 mmol) in THF (5 mL). Then the mixture was stirred under reflux for 15 h. After storage at room temperature overnight the Et_3NHCl precipitate was filtered off and washed with THF (6 mL). From the filtrate the solvent was removed *in vacuo*, and the residue was dissolved in $CDCl_3$ for an initial NMR analysis. Thereafter the solvent was removed *in vacuo*, and the red residue was dissolved in diethyl ether (1 mL) and pentane (1 mL). This solution was stored at 4 °C for several days, whereupon a first fraction of crystals had formed. X-Ray diffraction analysis confirmed their identity as disiloxane (LH)Ph*t*BuSi-O-SiPh*t*Bu(LH). The supernatant was transferred into a new Schlenk tube and stored at 4 °C for further 3 weeks to yield red crystals of LSiPh*t*Bu, which were separated from the solution by decantation and dried *in vacuo*. Yield: 0.075 g (0.22 mmol, 11.5 %). M. p. > 230 °C (decomposition). – UV/Vis ($CHCl_3$): λ_{max} (lg ε_{max}) = 359.8 nm (3.72), 472.9 nm (4.32). – ^1H NMR (400 MHz, $CDCl_3$): δ = 0.93 (s, 9 H, $(CH_3)_3C$), 6.53 – 6.55 (m, 1 H, ar), 6.76 (t, J = 7.6 Hz, 1 H, ar), 6.91 (d, J = 8.4 Hz, 1 H, ar), 7.07 – 7.10 (mm, 2 H, ar), 7.26 – 7.30 (mm, 5 H, ar), 7.54 – 7.56 (mm, 2 H, ar), 8.60 (s, 1 H, N=C-H). – $^{13}C\{^1H\}$ NMR (100 MHz, $CDCl_3$): δ = 21.7 ($(CH_3)_3C$), 28.3 ($(CH_3)_3C$), 111.5, 114.5, 117.3, 117.4, 120.4, 127.3, 127.8, 128.7, 128.9, 135.0, 135.6, 140.9, 144.2 (ar), 154.4 (C=N). – $^{29}Si\{^1H\}$ NMR (79.5 MHz, $CDCl_3$): $\delta = -72.2$. – $C_{21}H_{22}N_2OSi$ (346.5): calcd. C 72.79, H 6.40, N 8.08; found C 72.38, H 6.52, N 7.80.

LSiPhCy

LSiPhCy was obtained following the procedure described for $LSiMe_2$. Starting materials: Ligand LH_2 (0.33 g,

Table 6. Crystal structure data for LSiPh*t*Bu, (LH)Ph*t*BuSi-O-SiPh*t*Bu(LH), $LSiPh_2$ and L_2Si.

	LSiPh*t*Bu	**(LH)Ph*t*BuSi-O-SiPh*t*Bu(LH)**	**$LSiPh_2$**	**L_2Si**
Formula	$C_{21}H_{22}N_2OSi$	$C_{42}H_{46}N_4O_3Si_2$	$C_{23}H_{18}N_2OSi$	$C_{22}H_{16}N_4O_2Si$
M_r	346.50	711.01	366.48	396.48
T, K	296(2)	296(2)	296(2)	90(2)
Crystal size, mm^3	$0.60 \times 0.20 \times 0.05$	$0.26 \times 0.12 \times 0.04$	$0.45 \times 0.24 \times 0.22$	$0.14 \times 0.12 \times 0.07$
Crystal system	triclinic	triclinic	orthorhombic	tetragonal
Space group	$P\bar{1}$	$P\bar{1}$	*Pbca*	$P4_1$
a, Å	9.0899(14)	9.9444(3)	9.5504(2)	10.9255(3)
b, Å	12.067(2)	11.2545(3)	16.9266(4)	10.9255(3)
c, Å	17.595(3)	19.4439(8)	22.7329(5)	62.141(4)
α, deg	85.207(8)	92.260(2)	90	90
β, deg	86.712(9)	91.666(2)	90	90
γ, deg	88.912(8)	111.796(2)	90	90
V, Å^3	1919.9(5)	2016.76(12)	3674.91(14)	7417.6(6)
Z	4	2	8	16
D_{calcd}, g cm^{-3}	1.20	1.17	1.33	1.42
μ (MoK_α), cm^{-1}	0.1	0.1	0.1	0.2
F(000), e	736	756	1536	3296
hkl range	$-11 \le h \le +11$ $-15 \le k \le +13$ $-22 \le l \le +22$	$-11 \le h \le +11$ $-13 \le k \le +13$ $-22 \le l \le +23$	$-12 \le h \le +11$ $-21 \le k \le +21$ $-25 \le l \le +29$	$-13 \le h \le +6$ $-11 \le k \le +12$ $-52 \le l \le +73$
θ_{max}, deg / $(\sin\theta/\lambda)_{max}$, Å^{-1}	27.5 / 0.65	25.0 / 0.59	27.5 / 0.65	25.0 / 0.59
Refl. measured / unique	44727 / 8707	17886 / 7094	22159 / 4176	22936 / 11661
R_{int}	0.0372	0.0372	0.0261	0.0560
Param. refined	451	460	244	1046
$R(F)/wR(F^2)$[a] [$I \ge 2\sigma(I)$]	0.0422 / 0.1094	0.0471 / 0.0979	0.0372 / 0.1044	0.0545 / 0.1065
$R(F)/wR(F^2)$[a] (all data)	0.0732 / 0.1203	0.1112 / 0.1127	0.0561 / 0.1123	0.0708 / 0.1140
x (Flack)	–	–	–	−0.03(16)
GoF (F^2)[a]	1.048	0.940	1.077	0.999
$\Delta\rho_{fin}$ (max/min), e Å^{-3}	0.300 / −0.251	0.201 / −0.178	0.298 / −0.235	0.321 / −0.269

[a] Definition of R values and GoF, as well as information on weighting scheme applied: $R(F) = \Sigma(||F_o| - |F_c||)/\Sigma|F_o|$ for the observed reflections $[F^2 \ge 2\sigma(F^2)]$. $wR(F^2) = \{\Sigma[w(F_o^2 - F_c^2)^2]/\Sigma w(F_o^2)^2\}1/2$; $\mathrm{GoF}(F^2) = \{\Sigma[w(F_o^2 - F_c^2)^2]/(n-p)\}1/2$, ($n$ = number of reflections, p = number of parameters) with $w = 1/[s^2(F_o^2) + (AP)^2 + BP]$ where $P = (F_o^2 + 2F_c^2)/3$.

1.8 mmol) in THF (5 mL); cyclohexylphenyldichlorosilane (0.48 g, 1.9 mmol) and triethylamine (0.54 g, 5.4 mmol) in THF (5 mL). (Attempts to crystallize LSiPhCy, *e. g.*, from diethyl ether or pentane or mixtures thereof, failed so far). – $^{29}Si\{^1H\}$ NMR (79.5 MHz, $CDCl_3$): δ = −75.7.

$LSiPh_2$

A solution of LH_2 (0.31 g, 1.7 mmol) in THF (5 mL) was added dropwise to a solution of diphenyldichlorosilane (0.44 g, 1.8 mmol) and triethylamine (0.34 g, 3.4 mmol) in THF (5 mL). After stirring the mixture at r. t. for 1 h the precipitate was filtered off and washed with THF (6 mL). From the orange filtrate the solvent was removed *in vacuo*, and the residue was dissolved in chloroform (1.5 mL), whereupon crystallization of $LSiPh_2$ commenced. The mixture was stored at 4 °C overnight. Then the crystals of $LSiPh_2$ were isolated by decantation and washed with a mixture of chloroform (1 mL) and hexane (1 mL). Yield: 0.26 g (0.71 mmol, 42.6 %). M. p. 154 °C. – UV/Vis ($CHCl_3$): $\lambda_{max}(\lg\varepsilon_{max})$ = 352.3 nm (3.67), 470.4 nm (4.29). – ^1H NMR (400 MHz, $CDCl_3$): δ = 6.56 (s, 1 H, ar), 6.77 (t, J = 7.6 Hz, 1 H, ar), 7.02 (d, J = 7.6 Hz, 2 H, ar), 7.09 – 7.12 (m, 2 H, ar), 7.23 – 7.32 (m, 7 H, ar), 7.49 (d, J = 7.6 Hz, 4 H, ar), 8.54 (s, 1 H, N=C-*H*). – $^{13}C\{^1H\}$ NMR (100 MHz, $CDCl_3$): δ = 112.1, 115.1, 118.1 (2x), 121.0, 127.7, 128.1, 128.6, 129.0, 134.4, 135.0, 139.7, 139.8, 144.3 (ar), 153.7 (C=N). – $^{29}Si\{^1H\}$ NMR (79.5 MHz, $CDCl_3$): δ = −85.5. – $C_{23}H_{18}N_2OSi$ (366.5): calcd. C 75.37, H 4.95, N 7.63; found C 75.16, H 5.20, N 7.80.

L_2Si

0.56 g (3.03 mmol) LH_2 was dissolved in chloroform (6.5 mL) and added dropwise to a solution of silicon tetrachloride (0.27 g, 1.59 mmol) and triethylamine (0.64 g, 6.36 mmol) in chloroform (5 mL). The mixture was stored at r. t. for 8 weeks. The brown precipitate, which had formed within this time, was filtered off and washed with small amounts of chloroform and dried *in vacuo*. Yield: L_2Si 0.24 g, 40 %. M. p. > 320 °C (decomposition). – UV/Vis ($CHCl_3$): $\lambda_{max}(\lg\varepsilon_{max})$ = 338 nm (4.12), 464 nm (4.60). –

^{1}H NMR (400 MHz, $CDCl_3$): δ = 6.15 – 6.17 (m, 2 H, ar_{Pyrrol}), 6.64 (s, 2 H, ar_{Pyrrol}), 6.78 (d, J = 8.0 Hz, 2 H, ar), 6.83 (m, 2 H, ar), 6.88 – 6.89 (m, 2 H, ar_{Pyrrol}), 7.09 (m, 2 H, ar), 7.40 (dd, ^3J = 7.8, ^4J = 1.0 Hz, 2 H, ar). – $^{13}C\{^1H\}$ NMR (100 MHz, $CDCl_3$): δ = 112.7, 116.1, 116.6, 118.3, 119.9, 128.4, 128.8, 131.7, 133.0, 141.7 (ar), 152.5 (C=N). – $^{29}Si\{^1H\}$ NMR (79.5 MHz, $CDCl_3$): δ = −160.3. – $C_{22}H_{16}N_4O_2Si$ (396.5): calcd. C 66.65, H 4.07, N 14.13; found C 66.63, H 4.05, N 13.66.

Crystal structure determinations

Data were collected on Bruker Apex II diffractometer equipped with a CCD area detector using graphite-monochromated MoK_α radiation (λ = 0.71073 Å). The structures were solved by Direct Methods (SHELXS [16]) and refined by full-matrix least-squares methods on F^2 (SHELXL [17]) with anisotropic displacement parameters for the non-hydrogen atoms. The hydrogen atoms on carbon were refined isotropically in idealized positions. The hydrogen atoms bound to the nitrogen atoms were found by analysis of the residual electron density and were refined isotropically without bond length restraints. Selected parameters of data collection and structure refinement are summarized in Table 6.

CCDC 744885 (LSiPh*t*Bu), CCDC 744883 ($LSiPh_2$), CCDC 744884 ((LH)Ph*t*BuSi-O-SiPh*t*Bu(LH)) and CCDC 744882 (L_2Si) contain the supplementary crystallographic data for this paper. These data can be obtained free of charge from The Cambridge Crystallographic Data Centre *via* www.ccdc.cam.ac.uk/data_request/cif.

Acknowledgement

D. G. is grateful to Deutscher Akademischer Austausch Dienst (DAAD) for the award of a scholarship.

[1] For reviews on hypercoordinate silicon compounds see for example: a) D. Kost, I. Kalikhman, *Acc. Chem. Res.* **2009**, *42*, 303 – 314; b) D. Kost, I. Kalikhman, *Adv. Organomet. Chem.* **2004**, *50*, 1 – 106; c) R. Tacke, M. Pülm, B. Wagner, *Adv. Organomet. Chem.* **1999**, *44*, 221 – 273; d) C. Chuit, R. J. P. Corriu, C. Reye, J. C. Young, *Chem. Rev.* **1993**, *93*, 1371 – 1448.

[2] For recent publications dealing with hypercoordinate silicon compounds see for example: a) A. Kämpfe, E. Kroke, J. Wagler, *Eur. J. Inorg. Chem.* **2009**, 1027 – 1035; b) K. Lippe, D. Gerlach, E. Kroke, J. Wagler, *Organometallics* **2009**, *28*, 621 – 629; c) G. W. Fester, J. Wagler, E. Brendler, U. Böhme, D. Gerlach, E. Kroke, *J. Am. Chem. Soc.* **2009**, *131*, 6855 – 6864; d) J. Wagler, G. Roewer, D. Gerlach, *Z. Anorg. Allg. Chem.* **2009**, *635*, 1279 – 1287; e) E. Brendler, T. Heine, A. F. Hill, J. Wagler, *Z. Anorg. Allg. Chem.* **2009**, *635*, 1300 – 1305; f) E. Kertsnus-Banchik, E. Sela, J. Wagler, I. Kalikhman, D. Kost, *Z. Anorg. Allg. Chem.* **2009**, *635*, 1321 – 1325; g) S. Metz, C. Burschka, R. Tacke, *Chem. Asian J.* **2009**, *4*, 581 – 586; h) S. Metz, C. Burschka, R. Tacke, *Organometallics* **2009**, *28*, 2311 – 2317; i) B. Theis, S. Metz, F. Back, C. Burschka, R. Tacke, *Z. Anorg. Allg. Chem.* **2009**, *635*, 1306 – 1312; j) I. Kalikhman, E. Kertsnus-Banchik, B. Gostevskii, N. Kocher, D. Stalke, D. Kost, *Organometallics* **2009**, *28*, 512 – 516; k) S. Yakubovich, B. Gostevskii, I. Kalikhman, D. Kost, *Organometallics* **2009**, *28*, 4126 – 4132; l) E. P. A. Couzijn, J. C. Slootweg, A. W. Ehlers, K. Lammertsma, *Z. Anorg. Allg. Chem.* **2009**, *635*, 1273 – 1278; m) F. Riedel, A. Oehlke, S. Spange, *Z. Anorg. Allg. Chem.* **2009**, *635*, 1335 – 1340; n) A. Bockholt, P. Jutzi, A. Mix, B. Neumann, A. Stammler, H. -G. Stammler, *Z. Anorg. Allg. Chem.* **2009**, *635*, 1326 – 1334; o) M. Yamamura, N. Kano, T. Kawashima, *Z. Anorg. Allg. Chem.* **2009**, *635*, 1295 – 1299; p) A. R. Bassindale, D. J. Parker, P. G. Taylor, R. Turtle, *Z. Anorg. Allg. Chem.* **2009**, *635*, 1288 – 1294; q) E. P. A. Couzijn, D. W. F. van den Engel, J. C. Slootweg, F. J. J. de Kanter, A. W. Ehlers, M. Schakel, K. Lammertsma, *J. Am. Chem. Soc.* **2009**, *131*, 3741 – 3751.

[3] a) J. Wagler, G. Roewer, *Z. Naturforsch.* **2006**, *61b*, 1406 – 1412; J. Wagler, U. Böhme, G. Roewer, *Organometallics* **2004**, *24*, 6066 – 6069; c) J. Wagler, T. Doert, G. Roewer, *Angew. Chem.* **2004**, *116*, 2495 – 2498; *Angew. Chem. Int. Ed.* **2004**, *43*, 2441 – 2444.

[4] a) M. Yamamura, N. Kano, T. Kawashima, T. Matsumoto, J. Harada, K. Ogawa, *J. Org. Chem.* **2008**, *73*, 8244 – 8249; b) J. Wagler, G. Roewer, *Inorg. Chim. Acta* **2007**, *360*, 1717 – 1724; c) J. Wagler, D. Gerlach, U. Böhme, G. Roewer, *Organometallics* **2006**, *25*, 2929 – 2933; d) S. Yamaguchi, S. Akijama, K. Tamao, *J. Organomet. Chem.* **2002**, *652*, 3 – 9; e) I. El-Sayed, Y. Hatanaka, S. Onozawa, M. Tanaka, *J. Am. Chem. Soc.* **2001**, *123*, 3597 – 3598.

[5] a) K. Lippe, D. Gerlach, E. Kroke, J. Wagler, *Inorg. Chem. Commun.* **2008**, *11*, 492 – 496; b) G. González-García, J. A. Gutiérrez, S. Cota, S. Metz, R. Bertermann, C. Burschka, R. Tacke, *Z. Anorg. Allg. Chem.* **2008**, *634*, 1281 – 1286; c) J. Wagler, A. F. Hill, *Organometallics* **2008**, *27*, 6579 – 6586; d) D. Gerlach, E. Brendler, T. Heine, J. Wagler, *Organometallics* **2007**, *26*, 234 – 240; e) J. Wagler, D. Gerlach, G. Roewer, *Inorg. Chim. Acta* **2007**, *360*, 1935 – 1942.

[6] a) J. A. Castro, J. Romero, J. A. Garcia-Vazquez, A. Macias, A. Sousa, U. Englert, *Polyhedron* **1993**,

12, 1391 – 1397; b) N. Koprivanac, A. Metes, S. Papic, b. Kralj, *Spectroscopy Letters* **1996**, *29*, 27 – 39; c) B. Emanti, P. Indrani, R. J. Butcher, G. Rosair, S. Bhattacharya, *J. Chem. Sci.* **2005**, *117*, 167 – 173; d) S. Sawusch, N. Jäger, U. Schilde, E. Uhlemann, *Struct. Chem.* **1999**, *10*, 105 – 119.

[7] C. Hillairet, G. Michaud, S. Sirol, Eur. Pat. Appl., PCT/EP 2007/062112, WO 2008/061901 A1, **2008**.

[8] a) H. A. Tayim, A. S. Salameh, U. S. I. Meri, *Polyhedron* **1986**, *5*, 1509 – 1511; b) H. A. Tayim, A. S. Salameh, *Polyhedron* **1986**, *3*, 691 – 693; c) F. Capitan, L. F. Capitan-Vallvey, P. Espinosa, F. Molina, *Quimica Analitica (Barcelona, Spain)* **1985**, *4*, 335 – 345.

[9] H. Jiang, A. K. Kakkar, A. Lebuis, H. Zhou, G. K. Wong, *J. Mater. Chem.* **1996**, *6*, 1075 – 1077.

[10] A. W. Hanson, A. W. McCulloch, A. G. McInnes, *Can. J. Chem.* **1986**, *64*, 1450 – 1457.

[11] Q. Liu, M. Ding, Y. Lin, Y. Xing, *Acta Cryst.* **1998**, *54*, 145 – 146.

[12] O. Seiler, C. Burschka, S. Metz, M. Penka, R. Tacke, *Chem. Eur. J.* **2005**, *11*, 7379 – 7386.

[13] C. Pettinari, F. Marchetti, R. Pettinari, D. Martini, A. Drozdov, S. Troyanov, *Inorg. Chim. Acta* **2001**, *325*, 103 – 114.

[14] a) J. Wagler, *Organometallics* **2007**, *26*, 155 – 159; b) J. Wagler, E. Brendler, *Z. Naturforsch.* **2007**, *62b*, 225 – 234.

[15] M. J. Frisch, G. W. Trucks, H. B. Schlegel, G. E. Scuseria, M. A. Robb, J. R. Cheeseman, J. A. Montgomery, Jr., T. Vreven, K. N. Kudin, J. C. Burant, J. M. Millam, S. S. Iyengar, J. Tomasi, V. Barone, B. Mennucci, M. Cossi, G. Scalmani, N. Rega, G. A. Petersson, H. Nakatsuji, M. Hada, M. Ehara, K. Toyota, R. Fukuda, J. Hasegawa, M. Ishida, T. Nakajima, Y. Honda, O. Kitao, H. Nakai, M. Klene, X. Li, J. E. Knox, H. P. Hratchian, J. B. Cross, C. Adamo, J. Jaramillo, R. Gomperts, R. E. Stratmann, O. Yazyev, A. J. Austin, R. Cammi, C. Pomelli, J. W. Ochterski, P. Y. Ayala, K. Morokuma, G. A. Voth, P. Salvador, J. J. Dannenberg, V. G. Zakrzewski, S. Dapprich, A. D. Daniels, M. C. Strain, O. Farkas, D. K. Malick, A. D. Rabuck, K. Raghavachari, J. B. Foresman, J. V. Ortiz, Q. Cui, A. G. Baboul, S. Clifford, J. Cioslowski, B. B. Stefanov, G. Liu, A. Liashenko, P. Piskorz, I. Komaromi, R. L. Martin, D. J. Fox, T. Keith, M. A. Al-Laham, C. Y. Peng, A. Nanayakkara, M. Challacombe, P. M. W. Gill, B. Johnson, W. Chen, M. W. Wong, C. Gonzalez, J. A. Pople, GAUSSIAN 03 (revision C.02), Gaussian, Inc., Wallingford, CT (USA) **2004**.

[16] G. M. Sheldrick, SHELXS-97, Program for the Solution of Crystal Structures, University of Göttingen, Göttingen (Germany) **1997**. WINGX version: G. M. Sheldrick, release 97-2.

[17] G. M. Sheldrick, SHELXL-97, Program for the Refinement of Crystal Structures, University of Göttingen, Göttingen (Germany) **1997**. WINGX version: G. M. Sheldrick, release 97-2. See also: G. M. Sheldrick, *Acta Crystallogr.* **2008**, *A64*, 112 – 122.